Variable Structure Direct Torque Control of Encoderless Synchronous Reluctance Motor Drives with Maximized Efficiency

H. Abootorabi Zarchi[1], J. Soltani[2], Gh. R. Arab Markadeh[3], M. Fazeli[4], A. Kh. Sichani[5]

[1]*Faculty of Electrical & Computer Engineering, Isfahan University of Technology, Isfahan, Iran, abootorabi9@yahoo.com*

[2]*Faculty of Engineering, Azad University of Khomeini-shahr Branch, Khomeini-shahr, Isfahan-Iran, j1234sm@cc.iut.ac.ir*

[3,5]*Department of Engineering, Shahrekord University, Shahrekord, Iran, arab-gh@eng.sku.ac.ir, arash_kho@hotmail.com*

[4]*Faculty of Engineering, University of Malaya, Kuala-Lumpur, Malaysia, fazeli2003@yahoo.com*

***Abstract*- In this paper, a flexible DTC based on variable structure approach and space vector modulation is presented for encoderless Synchronous Reluctance Motor (SynRM) Drives. According to this method, a sliding mode-plus-PI controller is designed for torque and flux control in stator flux reference frame, respectively. The proposed controller is able to reduce the torque, flux, current and speed pulsations during steady-state behavior while the fast response and robustness merits of the classic DTC are preserved. In addition, an on-line adaptive loss minimization controller (ALMC) for SynRM drives is introduced. The ALMC provides a novel pattern of change in stator flux magnitude to achieve a minimum motor input power at any operating condition. The operating of the ALMC results in a smooth and fast loss minimization. Very low speed estimation (5 r/min) is satisfied by the elimination of the voltage sensors' dc offset. The simulation and experimental results obtained verify that the encoderless efficiency-optimized VS-DTC proposed for SynRM drives presents a good performance with minimized number of dependent parameters.**

***Keywords*—** Synchronous Reluctance Motor, Direct Torque Control, Sliding Mode, Encoderless, Eficiency-Optimized Strategy

I. INTRODUCTION

The SynRM is one of the oldest and simplest types of electric motors. In recent years, it has been shown that SynRM can be competitive with other ac motors [1-3]. A multitude of solutions for control of SynRM drives have been proposed [1]–[7]. Among them, the direct torque and stator flux control for SynRM drives has been developed as direct torque control (DTC) [4-7]. The DTC strategy was an induction motor control technique [8] that has been successful because it explicitly considers the variable structure nature of the voltage source inverter and uses few machine parameters, while being more robust to parameter uncertainty than field-oriented control (FOC) [9]. The DTC features fast responses, structural simplicity and robustness to modeling uncertainty and disturbances. DTC has some disadvantages that can be summarized in the following points: high torque, flux and current ripples; variable switching frequency behavior and difficulty to control torque and flux at very low speed. To overcome the above drawbacks, some researchers have tried to propose some different DTC space vector modulation (SVM) techniques or to improve switching state patterns [6, 7]. In [6], a predictive direct torque control has been presented for encoderless SynRM which is able to operate at low speed. At low speed operation, the rotor angular position is estimated by injecting test voltage signals (TVSs) to detect the spatial orientations of existing position-dependent rotor anisotropies. However, the TVSs deteriorate the performance of the predictive algorithm, and they create some audible noise. The method of [6] is complicated and for each motor chosen it is required to obtain the motor inductances by off-line parameter identification methods. In [7], a nonlinear method capable of high dynamic torque regulation and efficiency optimization of SynRM has been described based on input-output feedback linearization (IOFL) DTC-SVM. In [7], the SynRM efficiency is optimized by using Lagrange's theorem [10]. Then, the efficiency optimization criterion and the motor torque are chosen as output variables. IOFL technique however, requires the full knowledge of the motor parameters with sufficient accuracy. In addition, two PI controllers employed in [7] that its coefficients should be properly adjusted.

Variable structure control (VSC) or sliding mode control (SMC) is an effective, high frequency switching control for nonlinear systems with uncertainties [11]. It features simple implementation, disturbance rejection, strong robustness and fast responses. Since power converters for ac drives are, by their nature, switching devices, it is worth considering VSC as a solution for generating discontinuous control laws. In fact, the classical DTC is a VSC scheme, excellently designed to match the eight-state, discrete nature of the voltage source inverter. Recently, several solutions that integrate the VSC and DTC principles (VS-DTC) within high performance drives have been proposed [12-13]. A VS-DTC IPMSM drive was presented in stationary reference frame [12]. Although the proposed controller assure the tracking of the torque and stator flux of IPMSM but, the fast switching may generate unexpected chattering. So, authors of [12] have suggested using saturation function instead of sign type. This function reduces chattering phenomenon, however produces steady-state error and drops transient system behavior. A VS-DTC for induction machine was proposed with stator flux oriented [13]. It employs a switching component and a linear PI regulator for torque and flux control respectively. This flexible DTC scheme takes advantage of the best features of linear control, smooth operation, and of VSC, robustness to perturbations.

In the last two decades, the on-line loss minimization control of adjustable speed drives (ASDs) has gained increasing attention due to the system parameter independency and ease of implementation [14-17].

978-1-4244-6392-3/10/$26.00 ©2010 IEEE

According to this method, a control variable, which affects the input power, is changed while seeking the minimum input power at the particular operating point. An on-line loss minimization control of SynRM drive was proposed in [14], seeking a combination of d and q-axis current components which provides minimum input power. A step change to a d-axis component of stator current reference was applied for the purpose of searching a minimum input power operating point. If the power reduces, another step change is applied to the control variable until the minimum input power is achieved. A great deal of effort has been directed towards the adjustment of the step size of the control variable [15, 16]. A important deficiency of the stepwise change in the control variable is the long time the controller takes to reach the minimum input power [14-21]. However, in many applications with frequent changes in the operating point (speed and torque), e.g. in electric vehicles, the steady state period is short. Therefore the controller does not have enough time to reach the minimum input power condition. Thus the on-line loss minimization is impractical. To overcome this problem, an on-line adaptive loss minimization controller for interior permanent magnet motor (IPMSM) drives was introduced in [17]. The controller provides a novel pattern of continuous change in d-axis stator current to achieve a minimum drive input power at any operating condition.

Regarding the VSC merits and the advantages of using the SVM, this paper presents VS-DTC solution for sensorless SynRM drives. Direct torque and flux control is achieved by means of VSC. The DTC transient and robustness merits are preserved and the steady-state behavior is much improved. In addition, the proposed scheme is independent on inherent parameter variation and not need position sensor. Furthermore, the on-line adaptive loss minimization controller (ALMC) introduced in [17] for vector control of IPMSMs, is employed and re-designed for DTC of SynRM drives. The controller provides a continuous change in stator flux to achieve a minimum motor input power at any operating condition. The operation of the controller resulted in a smooth and fast loss minimization. Accuracy of the stator flux estimation is crucial for direct torque controlled SynRM drive in very low speed range. When the stator flux linkage is estimated by integrating the stator-induced voltage $\lambda_s = \int (v_s - R_s i_s)\, dt + \lambda_{s0}$, even minor dc offsets in the voltage and current signals accumulate by integration to form a substantial offset in the estimated stator flux vector. In this paper a simple technique for elimination of voltage sensors' dc offset is presented. It is worthwhile to mention that the current sensors' dc offsets, seen on the measured currents, are negligible.

II. VS-DTC OF SENSORLESS SYNRM DRIVES

To preserve DTC transient and robustness merits, a sliding mode-plus-PI controller is designed for torque and flux control respectively. In fact, based on classic DTC concept, a variable structure controller for direct torque and stator flux regulation is exploited. Block diagram of the proposed efficiency-optimized VSC-DTC for sensorless SynRM drives is shown in Fig. 1. This drive is stator-flux oriented and stator-flux controlled. Control quantities are the torque T_e and the stator flux magnitude λ_s. Torque reference T_e^* is produced by an outer speed control loop, with a PI speed controller. The inner loop includes VS-DTC controller which calculates the most appropriate stator voltage vectors to drive the torque and flux to track their references. The control stator voltage signals have been limited before proceeding to SVM block, providing a solution for high resolution control and constant inverter switching frequency. The flux reference λ_s^* is set in accordance with the on-line loss minimization algorithm. The flux estimator block is implemented by integrating the stator-induced voltage and then estimated torque is calculated. Stator flux and torque control can be achieved taking into account the SynRM stator equation in stator flux reference frame

$$\bar{V}_s = R_s \bar{i}_s + \frac{d}{dt}\bar{\lambda}_s + j\hat{\omega}_{\lambda s}\bar{\lambda}_s \tag{1}$$

where $\bar{V}_s$ and $\bar{i}_s$ are the stator voltage and current, R_s is the stator resistance, and $\hat{\omega}_{\lambda s}$ is the estimated stator flux angular speed. The direct and quadrature components of (1) are

$$V_{sx} = R_s i_{sx} + \frac{d}{dt}\lambda_s \tag{2}$$

$$V_{sy} = R_s i_{sy} + \hat{\omega}_{\lambda s}\lambda_s \tag{3}$$

Under the assumed orientation, the develop torque is

$$T_e = 1.5P\lambda_s i_{sy} \tag{4}$$

If the stator flux is constant, it is evident that torque can be controlled by the imaginary component V_{sy}, the torque component of the voltage vector

$$V_{sy} = \frac{2R_s}{3P\lambda_s} T_e + \hat{\omega}_{\lambda s}\lambda_s \tag{5}$$

The estimated stator flux speed $\hat{\omega}_{\lambda s}$ is calculated in a stationary reference frame as follows

$$\hat{\omega}_{\lambda s} = \frac{d}{dt}\left(\tan^{-1}\frac{\lambda_{Qs}}{\lambda_{Ds}}\right) = \frac{\left(\lambda_{Ds} * \dot{\lambda}_{Qs} - \lambda_{Qs} * \dot{\lambda}_{Ds}\right)}{\lambda_s^2} = \frac{\left(\lambda_{Ds} * \left(v_{Qs} - R_s i_{Qs}\right) - \lambda_{Qs} * \left(v_{Ds} - R_s i_{Ds}\right)\right)}{\lambda_s^2} \tag{6}$$

where v_{Ds}, v_{Qs}, i_{Ds} and i_{Qs} are the voltage and currents values in stationary reference frame as well as λ_{Ds} and λ_{Qs} are the estimated direct and quadrature components of stator flux (λ_s) in stationary reference frame, and are calculated as

$$\lambda_{Ds} = \int \left(v_{Ds} - R_s i_{Ds}\right) dt \tag{7}$$

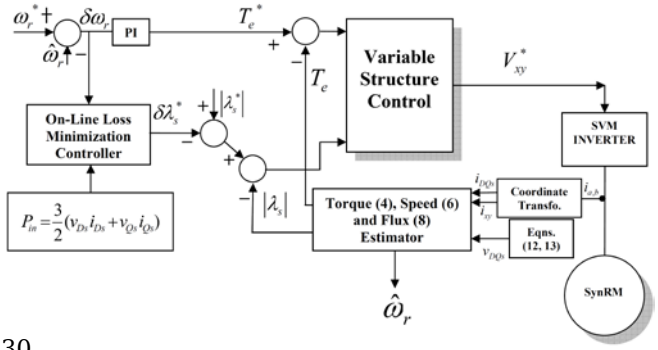

Fig. 1: The proposed efficiency-optimized VS-DTC for encoderless SynRM drives

$$\lambda_{Qs} = \int \left(v_{Qs} - R_s i_{Qs}\right) dt,\ \lambda_s = \sqrt{\lambda_{Ds}^2 + \lambda_{Qs}^2} \quad (8)$$

The flux control is accomplished by modifying the real component V_{sx}, the flux component of the voltage vector. For each sampling period T_{samp}, one can approximate the V_{sx} voltage as

$$V_{sx} = R_s\, i_{sx} + \Delta\lambda_s / T_{samp} \quad (9)$$

Since the computation of the $R_s\, i_{sx}$ voltage drop term requires a time-consuming stator flux coordinate transformation, a PI controller was used on the flux channel.

The block diagram of the torque and flux controller is shown in Fig. 2. It is named "linear and variable structure control" (LVSC) and consists of a sliding-mode controller that operates in parallel with a linear one. This controller is a generalized and flexible scheme which takes advantage of the best features of linear control, smooth operation, and of VSC, robustness to perturbations and modeling uncertainties.

The sliding surface $S = S_{\lambda s} + jS_{Te}$ is selected so as to impose sliding-mode operation with first-order dynamics

$$S = e_{\lambda s} + c_{\lambda s}\, s e_{\lambda s} + j\left(e_{Te} + c_{Te}\, s e_{Te}\right) \quad (10)$$

where $s = d/dt$, $e_{\lambda s} = \lambda_s^* - \lambda_s$, and $e_{Te} = T_e^* - T_e$ are the flux and torque errors, and T_e and λ_s denote the estimated quantities. Design constants $c_{\lambda s}$ and c_{Te} are selected so as to impose the desired linear first-order behavior of the system during sliding modes, i.e., when $S = 0$.

The controller (11) and (12) produces the reference voltage vector $V_s^* = V_{sx}^* + jV_{sy}^*$ in the stator flux reference frame

$$V_{sx}^* = \left(K_{P\lambda s} + K_{I\lambda s}/s\right)\left(e_{\lambda s} + K_{VSC\lambda s}\,\mathrm{sgn}(S_{\lambda s})\right) \quad (11)$$

$$V_{sy}^* = \left(K_{PTe} + K_{ITe}/s\right)\left(e_{Te} + K_{VSCTe}\,\mathrm{sgn}(S_{Te})\right) + \hat{\omega}_{\lambda s}\,\lambda_s \quad (12)$$

where $K_{P\lambda s}$, $K_{I\lambda s}$, K_{PTe} and K_{ITe} are the PI controller gains and $K_{VSC\lambda s}$, K_{VSCTe} are the VSC gains. An SVM block that generates the inverter switching signals is the output stage.

The LVSC employs a switching component and a linear one. During transients $e_\chi > K_{VSC\chi}\mathrm{sgn}(S_\chi)$, where χ is T_e or λ_s, and the linear (PI specific) behavior is dominant. In the steady-state, errors are very small and the switching (VSC specific) behavior prevails and the ripple magnitude depends on the K_{VSC} gains. Adequate balance between linear and switching behavior is easily achieved by proper gain selection. PI gains are selected so that the linear control provides the desired dynamic response, while the VSC gains determine the robustness in steady-state operation. the K_{VSC} gains are selected as large as needed to obtain the desired performance in terms of robustness and chattering.

III. Elimination of Voltage Sensors

In order to eliminate dc offset of voltage sensors, a simple method is introduced for estimating the phase voltages from the dc link voltage and the inverter switching state (**Sa, Sb, Sc**) [16]. However, the switching patterns in our practical setup are available in the complex programmable logic device (CPLD) and are applied to the PWM inverter with 1μs resolution (as is explained in section VI).

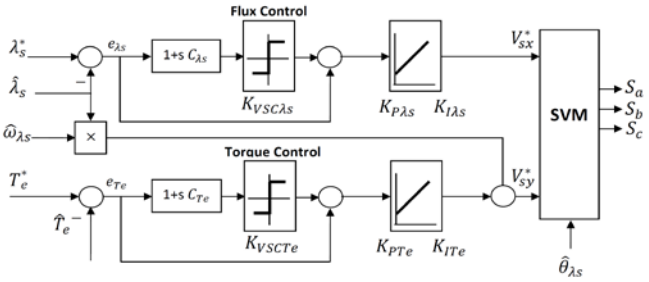

Fig.2: Linear and Variable Structure Control (LVSC) Block Diagram

To solve this problem, the average voltages of each phase in each sampling interval (5 kHz) are computed using the sector number of reference voltage space vector and timing assignment of SVM-PWM inverter which is available in the PC. Dependent on the sector number in which the inverter reference voltage vector is located in, the status of upper switch of each leg is seen in Table I. S_a, S_b and S_c refer to upper switch status of phase a, b and c, respectively. Considering Table I, the average of the inverter phase voltages during a sampling of T_s, is obtained as

$$\begin{pmatrix} v_{aN} \\ v_{bN} \\ v_{cN} \end{pmatrix} = \frac{V_{DC}}{T_s} * S_{ec_i} * \begin{pmatrix} t_1 \\ t_2 \end{pmatrix},\ i = 1,...,6;\ T_s = t_0 + t_1 + t_2 \quad (10)$$

Where V_{DC} is the inverter DC link voltage and letter "N" refers to negative polarity of DC link. t_1 and t_2 are the timing assignment and S_{eci} is i^{th} sector matrix which is obtained from Table I. As an example, S_{ec1} is 1st sector matrix.

$$S_{ec1} = \begin{pmatrix} 1 & 1 \\ 0 & 1 \\ 0 & 0 \end{pmatrix} \quad (11)$$

Now, the components of space voltage in two-axis stationary reference frame can be obtained as [18]

$$v_{Ds} = 2/3 * \left(v_{aN} - 0.5 * v_{bN} - 0.5 * v_{cN}\right) \quad (12)$$

$$v_{Qs} = 2/3 * \left(\sqrt{3}/2 * v_{bN} - \sqrt{3}/2 * v_{cN}\right) \quad (13)$$

One may note that zero time t_0 does not affect the components of stator voltage space vector (v_{Ds}, v_{Qs}) and therefore, the status of upper switch of each inverter leg during time t_0 is not seen in Table I and sector matrix.

Table I: Upper Switch Status of Each Inverter Leg Based on Sector Number

Sector NO.	1		2		3		4		5		6	
	t_1	t_2	t_1	t_2	t_1	t_2	t_1	t_2	t_1	t_2	t_1	t_2
Sa	1	1	1	0	0	0	0	0	0	1	1	1
Sb	0	1	1	1	1	1	1	0	0	0	0	0
Sc	0	0	0	0	0	1	1	1	1	1	1	0

S_{ec1} *Matrix*

IV. On-line Adaptive Loss Minimization Controller

In this section, the on-line adaptive loss minimization controller (ALMC) introduced in [17] for vector control of IPM drives, is employed and re-designed for DTC of sensorless SynRM drives to provide a continuous adjustment of stator flux reference amplitude for satisfying the efficiency-optimized criterion. The ALMC overcomes the major problem associated with the reported method based on step-change of control variable [14]. This is a long

search time to find the minimum loss condition. Therefore, the method is fast and smooth.

A. Basic Concepts

In the proposed ALMC the stepwise change of control variable is eliminated. Instead, it is replaced by a continuous adjustment of the control variable, stator flux level. A faster loss minimization is achieved by the continuous changes in the control variable since the relatively long transient period after each step change is avoided. The accuracy of the achievable minimum loss, in the stepwise methods, depends on the step size. The step size may be reduced as the input power reduces [15-17]. However, there is always a practical limit for the step size since the changes in the input power cannot be determined if a small step size is chosen.

In the proposed controller, the input power is monitored continuously inside a moving time window, similar to [17]. Therefore, as the control variable changes continuously, the change in the input power is determined at each instance by the difference between the two values at the beginning and at the end of the moving window. In this case, there is a limit for the size of window. However, since changes in both the control signal and input power occur continuously, a closer value to a true minimum power can be identified.

B. Design of ALMC

A simplified block diagram of the ALMC is shown in Fig. 3. This includes a power processing unit and a loss minimization algorithm (LMA). The processing unit receives one of the input signals to the ALMC, i.e. P_{in}, and finds out the change in the motor input power, δP_{in}, during the time window. The LMA, as the core of the ALMC, is responsible for making proper decisions based on the signals it receives, i.e. $\delta\omega_r$ and δP_{in}. It produces, in steady state, the ALMC output signal $\delta\lambda_s^*$, to adjust λ_s^* continuously towards its optimal value corresponding to a minimum P_{in}. These are explained in greater detail in the following.

Power Processing Unit: The signal P_{in} is subject to the averaging and filtering processes before it is applied to the ALMC. However, it requires further processing before it is used in the LMA. The power processing unit does this processing to find out a new signal δP_{in}. This signal represents the change of P_{in} over a certain time interval τ_d as it is needed by the ALMC.

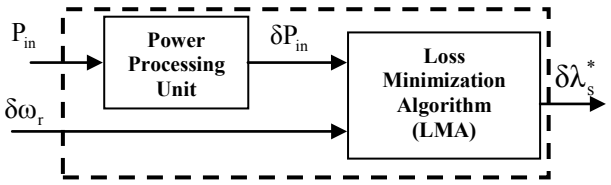

Fig. 3: Simplified Block Diagram of ALMC

The time interval τ_d is decided based on the desired smoothness of P_{in} and its sensitivity with respect to $\delta\lambda_s^*$. It is important to notice that δP_{in} is calculated at every sampling step. Therefore, it represents at each instance, the difference between the current and the n^{th} previous value of the motor input power as follows:

$$\delta P_{in}(k) = P_{in}(k) - P_{in}(k-n) \quad (14)$$

where n is found from $\tau_d = nT_{samp}$, and T_{samp} is the sampling time. The signal δP_{in} provides a natural way of monitoring the trend in the motor input power when λ_s^* is being changed by the ALMC**.** A negative value of δP_{in} indicates a falling input power while a positive value indicates a rising input power. Therefore, this can be used in search of an optimum stator flux level corresponding to a minimum P_{in}.

2) Loss Minimization Algorithm (LMA): the loss minimization algorithm is the core of ALMC. The algorithm monitors the two input signals $\delta\omega_r$ and δP_{in} all the time and generates the output signal $\delta\lambda_s^*$ correspondingly. Three main jobs are done by the LMA: the determination of the steady state speed, the direction test and the loss minimization.

The LMA monitors the motor speed error all the time. When the error is less than a small value for three measurements, with a fraction of second interval τ_ω, LMA detects a steady state speed. It is done by continuously keeping track of the current speed error sample $\delta\omega_r(k)$ and two previous speed error samples $\delta\omega_r(k\text{-}k_1)$ and $\delta\omega_r(k\text{-}2k_1)$, the number k_1 is found from $\tau_\omega = k_1 T_{s\omega}$ where $T_{s\omega}$ is the sampling time of the speed signal. The three speed error values are compared. If the difference between every two consecutive values is less than a speed error band $\Delta\omega_r$, the steady state speed is assured and the direction test is initiated. A small value for $\Delta\omega_r$ is desired. That way a smooth speed error signal needed by the ALMC is generated. Once the steady state speed is detected, the direction test starts. During this test, the signal $\delta\lambda_s^*$, which is originally equal to zero, changes incrementally or decrementally changes this in a exponential manner for a constant period of time equal to τ_d. Therefore, at the end of this period, δP_{in}, gives the amount of change in the input power caused by the change in $\delta\lambda_s^*$. If δP_{in} is less than a power band, ΔP_{in}, then the right direction for reducing P_{in} has already been chosen. Otherwise, the power reducing direction is the opposite direction. By this way, a proper direction is found regardless of the value of $\lambda_{sMax.}^*$, rated stator flux value. The value of power band determines the accuracy of ALMC. A smaller band requires a smoother δP_{in}.

After the loss minimizing direction is found, the LMA continues to make changes in $\delta\lambda_s^*$ with the same slope as long as the condition of $\delta P_{in} \le \Delta P_{in}$ is satisfied. During this period, P_{in} reduces smoothly and continuously until a very accurate minimum loss condition *is* achieved. The loss minimization period depends on the difference between rated stator flux command $\lambda_{sMax.}^*$ and the optimum value of λ_s^*. It also depends on the slope of the ramp which $\delta\lambda_s^*$ follows during the loss minimization.

The minimum loss condition is determined when a further change in the $\delta\lambda_s^*$ results in a value of δP_{in} greater than ΔP_{in}. At this point, the loss minimization period is terminated and

the direction of change in $\delta\lambda_s^*$ is reversed. Since the motor drive is working on the verge of the minimum loss condition now, a change in λ_s^* command along the new direction does not satisfy the condition of $\delta P_{in} \le \Delta P_{in}$. Therefore, the direction test is repeated in the opposite direction. Thus, the system enters a new mode of operation, the triangular mode, in which the direction test is repeated in an alternating direction and provides a triangular path for λ_s^*. This ensures minimum loss operation in case of gradual changes in motor operating condition. The operating point swings naturally in the vicinity of a true minimum loss condition.

3) Fast Dynamics: The dynamic performance of the motor drive may not be the best under the optimal Stator flux value. In order to provide desirable dynamics, a special software module is developed as part of the ALMC. The input to this module is the speed error signal, and the output is a disabling signal. This signal disables the ALMC if the absolute value of the speed error $\delta\omega_r$, exceeds a certain limit $\Delta\omega_r$. As a result, $\delta\lambda_s^*$ becomes zero and the stator flux command returns to its original maximum stator flux value $\lambda_{sMax.}^*$ to provide fast dynamics. The motor therefore undergoes a transient period with desirable dynamics provided by $\lambda_{sMax.}^*$. The ALMC remains disabled until the steady state speed is detected again.

V. Simulation Results

Some simulations are performed to show that the proposed VS-DTC drive is able to operate with reduced torque and flux ripple, without compromising the fast dynamic response and robustness of torque and flux control, of the classic DTC [8]. The VS-DTC and DTC strategies are simulated for a 0.37 Kw four-pole three-phase SynRM drive (for more information see Table I), at 5 KHz sampling frequency, and representative results are illustrated in Fig. 4. In both cases, at the instant 1 sec, the torque command is changed from -1 N.m to +1 N.m, with the stator flux maintained at the rated level, while the motor was running at 200 Rpm. The torque transients and stator flux magnitude in the VS-DTC drive are shown in Fig. 4.a, while Fig. 4.b shows similar quantities in the DTC drive. Although the DTC was fine tuned to produce low torque ripple, the VS-DTC exhibits much lower ripple, while its dynamic response is approximately the same. Torque response in Fig.4 illustrates well the characteristic behavior of the VS-DTC controller: it has linear behavior during transients, and switching behavior is apparent in the steady-state. Increasing the VSC gains strengthens the VSC component, increases the ripple, and makes the VS-DTC behavior approach that of DTC. The VS-DTC flux control is superior to DTC flux control, it has low ripple, and is equally robust with respect to torque transients.

Table I: Specifications and Parameters of three-phase SynRM

$P_n = 370W$	$V_n = 230$	$I_n = 2.8A$
$L_{md,unSat} = 232mH$	$L_{md,Sat} = 178mH$	$L_{mq} = 118mH$
$R_s = 2.95\Omega$	$f_n = 60$ Hz	$No.\ of\ Poles = 4$
$T_{en} = 1.9N.m$	$J_m = .015$ Kg.m^2	$B_m = .003$ Nm/rad/sec

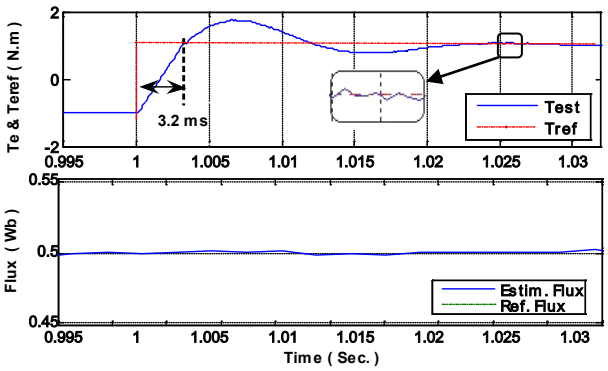

a) The proposed VS-DTC method

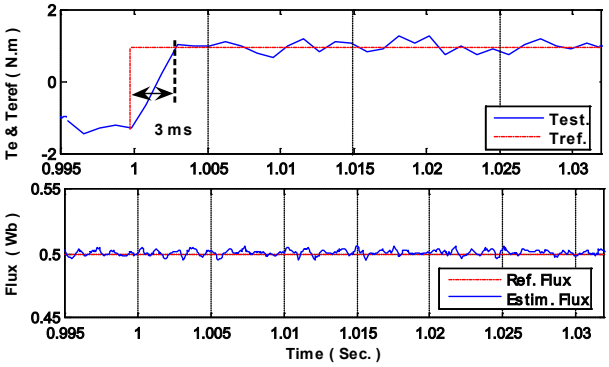

b) Classical DTC method

Fig.4: Torque Transients and Stator Flux magnitude (Simulation Results)

VI. Exprimental Setup and Results

For practical evaluation of the actual system performance, a PC-based prototype system was built and tested. The experimental setup corresponding to overall system block diagram shown in Fig. 1 including ALMC is depicted in Figs. 5 and 6 consists of the following sections: a 0.37kW three-phase SynRM and a 1.1kW DC generator as its load, Three-phase voltage source inverter and its isolation board, Voltage and current sensors board, 96 bit Advantech digital IO card; 32-channel Advantech A/D converter card; CPLD board and a personal computer (PC) for calculating required signals and viewing the registered waveforms. The SynRM parameters are reported in Table I.

The SynRM is supplied by a three-phase inverter with a symmetrical two level space vector modulation. A Xilinx XC95288xl CPLD has been selected for real time implementation of switching patterns using a switching frequency of 5 kHz. The CPLD board communicates with PC via the digital Advantech PCI-1753 I/O board. The inverter has been implemented specifically for this experiment using SKM75 GD 124 D SEMIKRON module. The required drive board has been designed by HCPL 316J which is fast and intelligent IGBT driver and guarantees a reliable isolation between the high voltage and control boards. The DC link voltage and stator phase currents and voltages are measured by Hall-type LEM sensors. All measured electrical signals are filtered and then converted to digital signals using an A/D card with 10μs conversion time. In order to evaluate the accuracy of rotor speed estimation, the actual rotor position is obtained from an absolute encoder with 1024 pulses per revolution.

A. Dynamics Performance

The torque and stator flux dynamic responses to command changes are presented in Fig. 7. The rise time for proposed

VS-DTC is 3.5 ms and in terms of settling time, estimated torque signal reaches steady-state within 10 ms. As shown in Fig. 7, the torque overshoot is acceptable.

B. Steady-State Performance

The steady-states of speed, torque and flux at 1400 rpm with 50% full load under proposed VS-DTC are shown in Fig. 8. From this figure, it can be seen the ripples in speed and torque are reduced significantly.

C. Chattering Free Responses

The chattering free torque and flux dynamics are illustrated in Fig. 9 when the torque command reverses between ±1 N.m. the corresponding trajectories of estimated rotor speed, flux and phase current are in this figure.

D. Very Low Speed Operation

The performance of the proposed rotor speed estimation method at very low speed has been shown in Fig. 10. The speed reference is reserved from -5 rpm to +5 rpm at t =10 Sec. under 50% full load. It is seen that the speed reference command is perfectly tracked and the torque and speed are smooth enough and flux hodograph is almost circle.

E. Drive Performance under the ALMC

Fig. 11 shows the experimental results of drive performance under the ALMC.

The motor is started under a low load condition in response to a medium step speed command as in Fig. 11.a. The original stator flux command is set at maximum value to provide fast dynamics. At about t = 2.0 seconds, a steady state speed is detected by the ALMC. Then, the direction test determines an decreasing direction for λ_s^*. Subsequently, the adjustment of λ_s^* is started towards its optimal value as shown in Fig. 11.b. After only about one second, the motor input power reaches its minimum value as shown in Fig. 11.c. This is about a 35% reduction in the motor input power. Then, the triangular mode of operation is initiated.

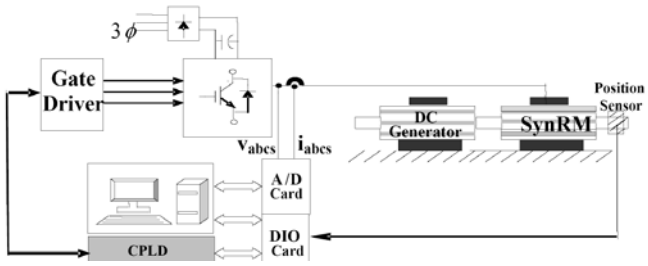

Fig. 5: Laboratory Implementation Block Diagram

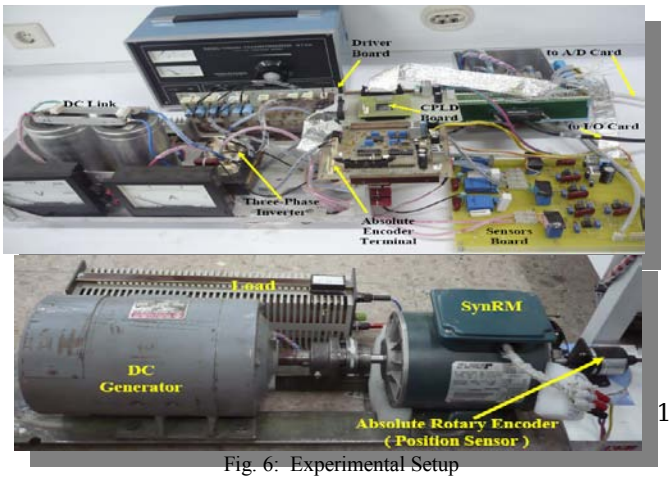

Fig. 6: Experimental Setup

The motor dynamics under ALMC are excellent, It is validated by applying a speed command change at t = 7 seconds. As a result, the ALMC is deactivated promptly, λ_s^* returns to its original value, $\lambda_{sMax.}^*$, and a new steady state speed is reached after a desirable transient period. The ALMC becomes active again, and a minimum input power is obtained at the new operating point.

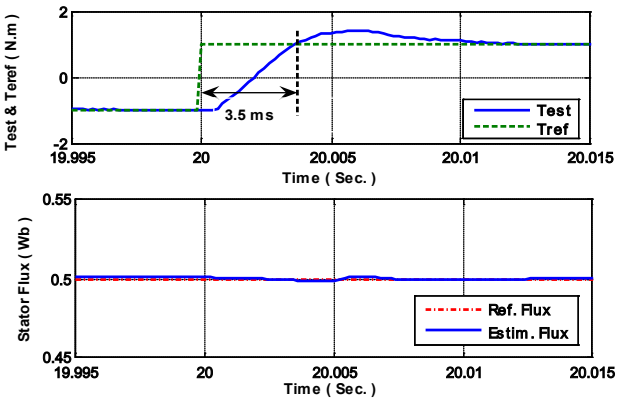

Fig.7: Dynamic Performance of VS-DTC. The motor was running at -200 Rpm with -1N.m Load before the Torque Changed to 1N.m

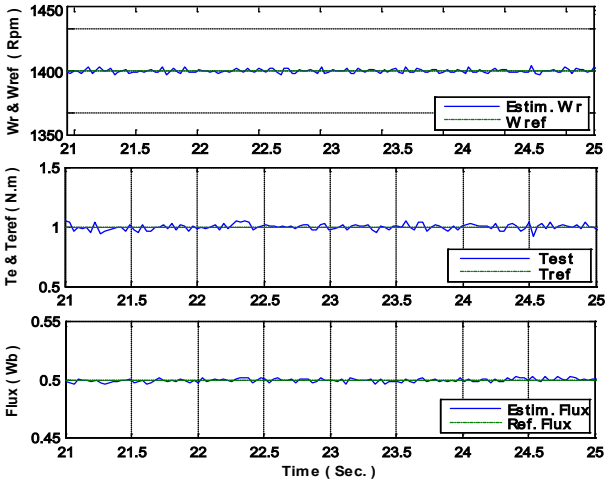

Fig.8: Steady-State Performance of VS-DTC, Speed, Torque and Flux at 1400 Rpm with 50% Full Load

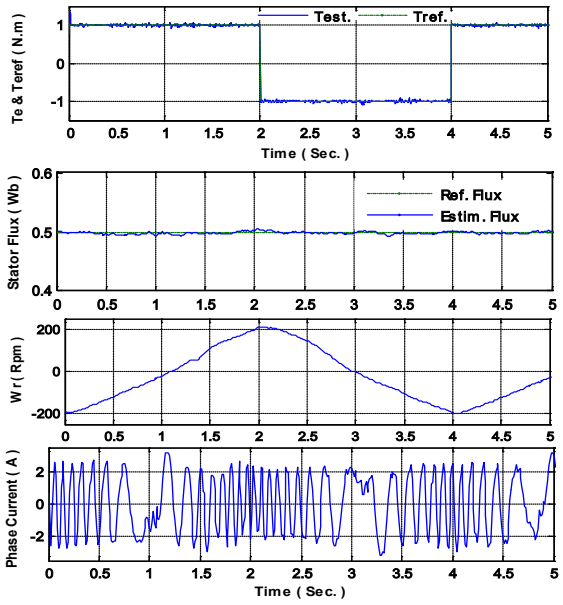

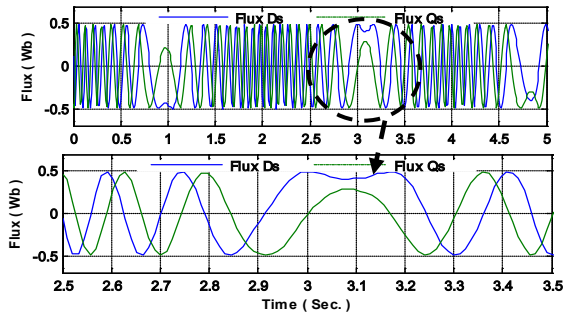

Fig. 9: Chattering Free Responses of SynRM Drive System under Proposed VS-DTC, when Torque Reverses.

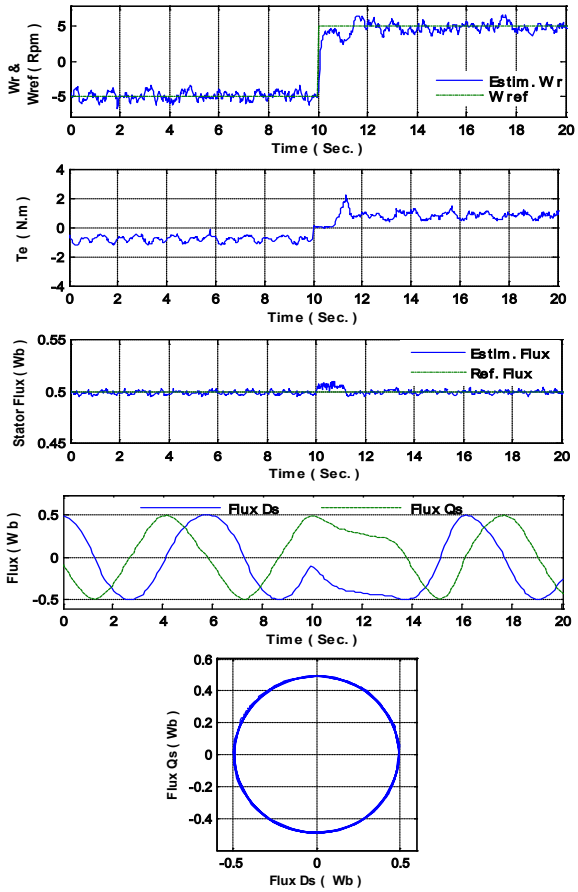

Fig. 10: Performance of the proposed method in very low speed

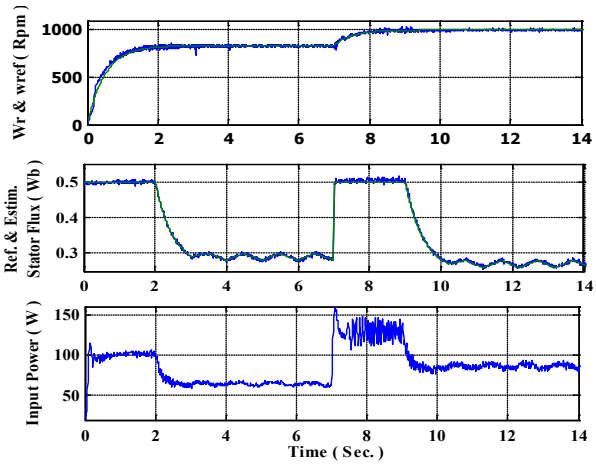

Fig. 11: Experimental results of drive performance under ALMC. a) Speed response, b) Reference and estimated stator fluxes, c) Motor input power.

VII. CONCLUSION

In this paper, combining the principles of the Sliding Mode, DTC, and space-vector modulation (SVM) yields a simple but robust direct torque control of a sensorless SynRM drive in stator flux reference frame. In particular, the sliding mode control contributes to robustness of the drive, the DTC results in a fast dynamic response, and the SVM improves the torque, flux and current steady-state waveforms by ripple reduction. In addition, an on-line adaptive loss minimization algorithm was introduced for SynRM drives. The algorithm minimizes the motor input power by a new pattern of change in stator flux amplitude so that the drive performance under the proposed ALMC is very smooth and fast. Based on this control approach, the rotor low speed estimation (5r/min) was also obtained.

REFERENCES

[1]. Lipo, T. A., 'Synchronous Reluctance Machines- A viable alternative for ac drives', *Electric Machines and Power Systems, 1991, vol. 19, pp. 659-671*

[2]. Hofmann, H.F., Sanders, S.R. and EL-Antably, A., "Stator-flux-oriented vector control of synchronous reluctance Machines with maximized efficiency", *IEEE Trans. On Ind. Elect., vol. 51, Issue 5, Oct. 2004, pp. 1066-1072*

[3]. Guglielmi, P., Pastorelli, M., Vagati, A, "Impact of cross-saturation in sensorless control of transverse-laminated synchronous reluctance motors", *IEEE Trans. On Ind. Elect., vol. 53, Issue 2, 2006, pp. 429-439*

[4]. R. Morales Caporal and M. Pacas, "Encoderless Predictive DTC for SynRM at Very Low and Zero Speed", *IEEE Trans. Ind. Elect., vol. 55, No. 12, Dec. 2008, pp. 4408-4416*

[5]. T. H. Liu and H. H. Hsu, "Adaptive Controller Design for a Synchronous Reluctance Motor Drive System with Direct Torque Control", *IET Electric Power Appl., Vol.1, No.5, 2007, pp. 815–824 815*

[6]. R. Morales Caporal and M. Pacas, "A Predictive Torque Control for the Synchronous Reluctance Machine taking into account the magnetic cross saturation", IEEE Trans. Ind. Elect., vol. 54, No. 2, 2007, *pp. 1161-1167*

[7]. H. D. Lee, S. J. Kang and S. K. Sul, "Efficiency-Optimized Direct Torque Control of Synchronous Reluctance Motor Using Feedback Linearization", IEEE Trans. on Ind. Elect., vol. 46, No. 1, pp 192-198, 1999es and Power Systems, vol. 19, 1991, pp. 659-671

[8]. I. Takahashi and N. Noguchi, "A New Quick Response and High Efficiency Control Strategy of an Induction Motor", IEEE Trans. Ind. Appl., Vol. 22, 1986, pp. 820-827

[9]. D. Casadi, F. Profumo, G. Serra and A. Tani, " FOC and DTC: Two Variable Schemes for Induction Motors Torque Control", IEEE Trans. Power Elec., Vol. 17, No. 5, Sept. 2002, pp. 779-787

[10]. Marino, R. and Tomei, P., 'Nonlinear Control Design', Prentice Hall, Inc, 1995

[11]. Hung, J.Y., Gao, W. and Hung, J.C., "Variable structure control: a survey**",** IEEE Trans. Ind. Elect., Issue 1, vol. 40, Feb. 1993, pp. 2-22

[12]. Z. Xu and M. F. Rahman, "Direct Torque and Flux Regulation of an IPM Synchronous Motor Drive Using Variable Structure Control Approach", IEEE Trans. On Power Elect., vol. 22, No.6 , Nov. 2007, pp. 2487-2498

[13]. C. Lascu, I. Boldea and F. Blaabjerg, " very Low Speed Variable Structure Control of Sensorless Induction Machine Drives without Signal Injection", IEEE Trans. Ind. Appl., vol. 41, No. 2, 2005, pp. 591-598

[14]. T. Matsuo, A. El-Antably and T.A. Lipo 'A New Control Strategy For Optimum Efficiency Operation of a Synchronous Reluctance Motor', Industry Applications Conference, 1996. Thirty-First IAS Annual Meeting, IAS '96, Vol. 1, 6-10 Oct., 1996,pp.109 – 116.

[15]. G.D.D. Sousa, B.K. Bose, and J.G. Cleland, "Fuzzy Logic Based On-Line Efficiency Optimization Control of an Indirect Vector-Controlled Induction Motor Drive" IEEE Trans., 1E-42, April 1995, pp. 192-198.

[16]. Holtz, J. and Quan, J., "Drift- and Parameter-Compensated Flux Estimator for Persistent Zero-Stator-Frequency Operation of Sensorless-Controlled Induction Motors", *IEEE Trans. On Ind. Appl., vol. 39, No. 4, July/Aug. 2003, pp. 1052-1060*

[17]. S. Vaez and M.A. Rahman, 'An on-line loss minimization controller for interior permanent magnet motor drives', IEEE Trans. On Energy Conv., Vol. 14, No. 4, December 1999, pp. 1435-1440.

[18]. Broeck, V. d., Skudelny, H. C. and Stanke, G. V., "Analysis and Realization of a Pulse Width Modulator Based on Voltage Space Vectors", *IEEE Trans. On Ind. Appl., vol. 24, No. 11, 1988, pp. 142-150*